PHYSICAL REVIEW B **87**, 214202 (2013)

# Inverse simulated annealing for the determination of amorphous structures

Jan H. Los and Thomas D. Kühne*
*Institute of Physical Chemistry and Centre for Computational Science, Johannes Gutenberg University Mainz, Staudinger Weg 7, D-55128 Mainz, Germany*

(Received 20 February 2013; revised manuscript received 21 April 2013; published 17 June 2013)

We present an efficient optimization method to determine the structure of disordered systems in agreement with available experimental data. Our approach permits the application of accurate electronic structure calculations within the structure optimization. This technique is demonstrated within density functional theory by the calculation of a model of amorphous carbon.

DOI: 10.1103/PhysRevB.87.214202 PACS number(s): 71.15.−m, 31.15.−p, 71.23.−k

Amorphous solids can be produced from almost any chemical system and are of great interest due to their large variety of technologically important applications. In addition to conventional silicate glasses, they are, for example, used in optical waveguides (oxides), plastics (organic polymers), solar cells (semiconductors), biomaterials (amorphous metals), xerography, and nonvolatile memory devices (chalcogenides), to name but a few.[1,2] Nevertheless, finding their atomic-scale structure is still a major challenge in material science[2–4] due to the absence of lattice periodicity and long-range-order characteristics of a crystalline solid. Many sophisticated modeling techniques from the field of crystal-structure prediction are based on searching the global minimum in the energy landscape for periodic structures.[5–13] However, an amorphous solid does not correspond to a global, but to a local, energy minimum, which is energetically low enough to stabilize the structure against alternative packings and exhibits desirable target properties.

The most commonly applied computational technique to obtain the amorphous structure is to slowly quench it from the melt by Monte Carlo (MC)- or molecular dynamics (MD)-based simulated annealing (SA).[14] However, the lack of exploitable symmetry and, therefore, large number of degrees of freedom requires the cooling to be conducted as slowly as possible to determine an approximation of the amorphous structure, and is, therefore, computationally very demanding. This is even more pronounced in conjunction with accurate *ab initio* electronic structure techniques, in spite of significant progress in recent years,[15,16] allowing for satisfactory structure determinations.[17–20]

Instead of performing an elaborate calculation to obtain an approximate amorphous model and to assess *a posteriori* how well it matches the experiment, McGreevy and co-workers demonstrated that it can be beneficial to reverse this procedure, hence the name reverse Monte Carlo (RMC).[21,22] Contrary to energy-based minimization techniques, this method aims at directly modeling the structure without invoking any computationally expensive potential-energy calculation, using only available experimental data. Specifically, the available experimental data are reproduced simply by minimizing a function of the form

$$\mathcal{F}(\mathbf{R}) = \sum_p w_p \left[\chi_p(\mathbf{R}) - \chi_p^{\mathrm{exp}}\right]^2 \qquad (1)$$

under variation of the atomic positions $\mathbf{R} = \{\mathbf{r}_i\}$ using the metropolis Monte Carlo method.[23] In Eq. (1), $\chi_p(\mathbf{R})$ and $\chi_p^{\mathrm{exp}}$ are the calculated and experimental values, respectively, of a property $p$, while $w_p = 1/\sigma_p^2$ is a weight factor and $\sigma_p$ is the experimental uncertainty for the corresponding property.

Even though $p$ can, in principle, be any arbitrary property, in practice, only geometric quantities, obtainable from neutron or x-ray scattering data such as the structure factor or the pair-correlation function for which $\chi_p(\mathbf{R})$ can be evaluated easily and quickly, are employed. In particular, typically no electronic quantities based on accurate electronic structure calculations are utilized, which would otherwise be computationally unfeasible. While on the one hand, RMC allows for an efficient and routine modeling of rather complex disordered structures, on the other hand, the resulting models are not necessarily physically sensible. It is, therefore, good practice to circumvent that as much as possible by imposing specifically selected constraints.[22,24–26] Although, eventually, this often leads to rather pleasing results, this may not be the case when studying unknown systems where good constraints are not known from the outset. In addition, since the atomic configuration in RMC is not relaxed into a local-energy minimum, the resulting structure is not necessarily stable.

The inverse design technique of Franceschetti and Zunger allows one to, at least partially, circumvent the shortcomings just mentioned by determining the crystal structure based on electronic structure properties, which are rather sensitive with respect to the atomic positions. In their method, an inner local geometry optimization is performed in each optimization step to relax the structure.[27] However, for the sake of efficiency, the latter is conducted using an empirical valence force field only.[28] Furthermore, in order to facilitate the calculation, they confine themselves to highly symmetric structures on a given crystal lattice.

In this work, we improve upon the existing approaches by proposing an efficient method, which we call inverse simulated annealing (ISA). This method combines the global minimization of a linear combination consisting of various geometric and electronic properties with structure relaxation to determine an amorphous solid in best agreement with available experimental data. Specifically, this is achieved by adding the potential energy $U(\mathbf{R})$ to the objective function of Eq. (1), and employing a modified hybrid Monte Carlo (HMC)-based SA scheme to minimize it. We will demonstrate that the present method is efficient enough to be applicable in conjunction with accurate electronic structure calculations, and in this way allows one to routinely determine the amorphous structure.

In the following, we will confine ourselves to effective single-particle theories, such as density functional theory

 

(DFT).[29] Hence, the modified objective function to be minimized reads as

$$\tilde{U}(\mathbf{R}) = U(\mathbf{R}) + \sum_p w_p\left[\chi_p(\mathbf{R}) - \chi_p^{\exp}\right]^2 + \sum_q w_q\left(\xi_q[\mathbf{R},\{\psi_i\}] - \xi_q^{\exp}\right)^2, \quad (2)$$

where $\tilde{U}(\mathbf{R})$ is a fictitious energy and $U(\mathbf{R})$ is the potential energy, as obtained by DFT, while $\xi_q[\mathbf{R},\{\psi_i\}]$ and $\xi_q^{\exp}$ are the computed and experimental values, respectively, of an electronic quantity $q$. Note that the variance to Eq. (1), $w_p$ and $w_q$, now acquire the dimensions of energy divided by the dimension of $\chi_p^2$ and $\xi_q^2$, respectively.

In minimizing $\tilde{U}(\mathbf{R})$, we take advantage of the fact that by using Eq. (2), the accessible phase space is substantially reduced and restricted to energetically low-lying configurations. In other words, even though the dimensionality of the phase space is equally vast, the optimization is guided in a funnel-like fashion towards the minimum of $\tilde{U}(\mathbf{R})$. Obviously, in spite of that, we still need a global optimization method to minimize Eq. (2) that is efficient enough to enable the calculation of $U(\mathbf{R})$ at the DFT level of theory. The fact that the derivatives of some of the properties in Eq. (2) with respect to $\mathbf{R}$ are not directly available and may not even exist due to possible discontinuities immediately suggests a MC-based minimization procedure.[30] The development of such a technique is therefore an essential part of the present work.

For the purpose of minimizing Eq. (2), while at the same time using as few electronic structure calculations as possible, we propose here a "fuzzy" HMC-based SA scheme within the *NVE* instead of the more common *NVT* ensemble that consists of only a single modified MD step. In comparison to standard MC- or MD-based SA techniques, we found that this technique performs particularly well as a minimization method, as will be shown. The positions and velocities of all atoms in each trial move are varied according to a slightly modified velocity-Verlet algorithm,

$$\begin{aligned}\mathbf{r}_i' &= \mathbf{r}_i + \mathbf{v}_i dt + \frac{1}{2}\frac{\tilde{\mathbf{f}}_i}{m_i}dt^2 \\ \mathbf{v}_i' &= C\left[\mathbf{v}_i + \frac{1}{2}\left(\frac{\tilde{\mathbf{f}}_i}{m_i} + \frac{\tilde{\mathbf{f}}_i'}{m_i}\right)dt\right],\end{aligned} \quad (3)$$

where $\mathbf{v}_i$ are the ionic velocities, $m_i$ are the nuclear masses, and $dt$ is a randomly chosen time step from a uniform distribution within the interval $[0, dt_{\max}]$, while the prime superscripts are used to indicate quantities of the new (trial) configuration. The forces $\tilde{\mathbf{f}}_i$ are the best possible estimate for $-\partial\tilde{U}/\partial\tilde{\mathbf{r}}_i$, i.e., omitting the contributions from those terms in the sums of Eq. (2) for which no derivatives are directly available. This and the presence of a maximum time step $dt_{\max}$, which is in general much larger than in standard MD and continuously adjusted to obtain an acceptance rate of about 50%, is why we call our modified HMC algorithm fuzzy. In order to ensure that the total energy is conserved, in Eq. (3) we have introduced an additional prefactor denoted as $C$, which was chosen in such a way that $1/2\sum_i^N m_i|\mathbf{v}_i'|^2 = K' = E - U'$ holds, where $K'$ is the kinetic energy of the system of the proposed trial configuration. Within the *NVE* ensemble, the probability of acceptance of a trial move is given by[31]

$$P = \min\left[1, \left(\frac{E-U'}{E-U}\right)^{3N/2-1}\right], \quad (4)$$

where $N$ is the number of atoms.

As already mentioned, the present approach differs from the standard HMC algorithm in the fact that the *NVE* instead of the usual *NVT* ensemble is employed. Furthermore, only a single MD step is taken in each HMC step and the velocities are not randomly reinitialized thereafter. The necessary random element in our HMC method comes from the randomly chosen, variable time step $dt$ instead. Whenever a HMC move is accepted, the positions and velocities are updated as $(\mathbf{r}_i,\mathbf{v}_i) = (\mathbf{r}_i',\mathbf{v}_i')$, just as in normal MD. Otherwise, if an HMC move is rejected, then one possibility is to maintain $(\mathbf{r}_i,\mathbf{v}_i)$, in which case no update is required. We will denote this straightforward version of our method as fHMC-*NVE*. However, regarding the efficiency of the minimization procedure, it is desirable to design an algorithm that combines a large time step with a high acceptance rate. It appears that an improvement in this direction is obtained by maintaining the velocities of the rejected configurations, i.e., by updating according to $(\mathbf{r}_i,\mathbf{v}_i) = (\mathbf{r}_i,\mathbf{v}_i')$ after a rejection. In this modified algorithm, indicated hereafter as mfHMC-*NVE*, the velocities are gradually turned in the direction of the forces upon repeated rejections. As a consequence, the acceptance probability for large displacements (i.e., large $dt$) increases, since the displacements become more and more parallel to the forces, i.e., the direction of decreasing potential energy.

To assess the performance of our HMC-based minimization technique, we have applied it to carbon using the empirical improved long-range carbon bond-order potential (LCBOPII).[32] This bond-order potential has been shown to accurately describe many carbon phases including the disordered, liquid phase within a whole range of different densities.[33] We have selected a system consisting of 216 atoms within a cubic simulation box with periodic boundary conditions, which corresponds to a density of $\rho = 3.1$ g/cm$^3$, which is in close agreement with the experimentally determined density of amorphous carbon.[34] For the sake of simplicity, in these simulations, which are meant to test and compare the performance of different minimization techniques, momentarily only the potential energy is minimized.

The applied total-energy schedule as a function of the (fictitious) MC "time" is schematically shown in Fig. 1(a). Starting at a high total energy $E = -1000$ eV, to create a well-disordered liquid phase, the schedule includes a liquid equilibration period at constant $E = -1200$ eV, after which the system is cooled down linearly to $E = -1450$ eV during a time interval $\Delta t_{\text{cool}}$. After that, the system is relaxed in a relatively short quench by further decreasing $E$ to a value close to the final potential energy $U_{f,0}(\mathbf{R})$. Note that the instantaneous temperature of the system can be deduced from $K = (3/2)Nk_BT = E - U$, which implies $T = 2(E-U)/(3Nk_B)$, so that $T \to 0$ K for $E \to U_{f,0}$.

The results for the average, final potential energy per atom at 0 K, $U_{f,0}(\mathbf{R})/N$, as a function of the cooling time interval $\Delta t_{\text{cool}}$ in units of total-energy evaluations (tee), based on 40 independent simulations, are shown in Fig. 1(c)

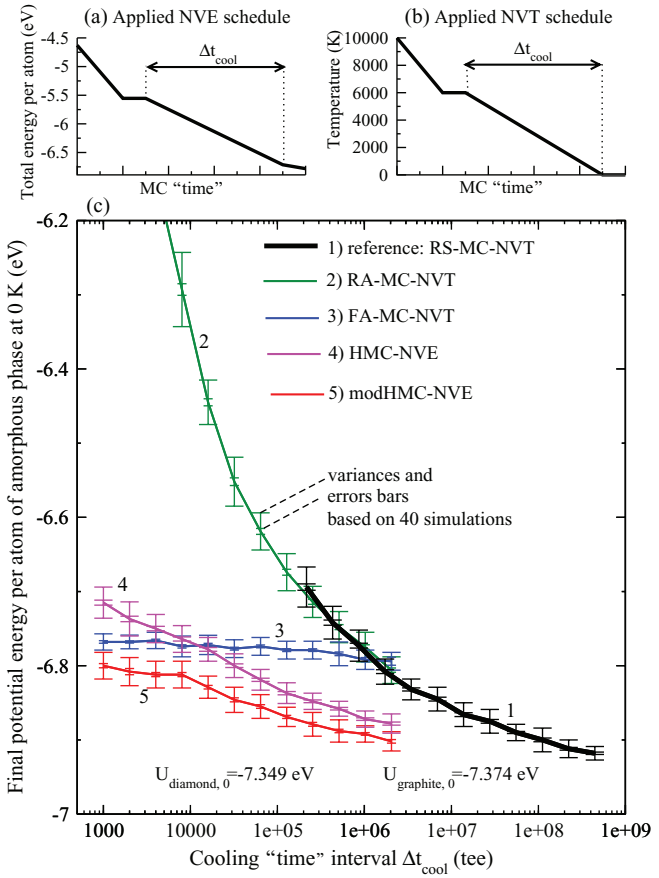


FIG. 1. (Color online) Comparison of the average over the final potential energies at 0 K of amorphous carbon as generated by the various minimization method as a function of the quenching time $\Delta t_{\text{cool}}$. The averages are based on 40 independent simulations, allowing for the calculation of variances and error bars as indicated. Note the logarithmic scale for the "time" axis.

and compared to the results from other, more standard minimization techniques. These include the reference, which is a random single-atom (RS) displacement MC method within the *NVT* ensemble, indicated as RS-MC-*NVT*, and two random all-atom (RA) MC methods within the *NVT* ensemble: the RA-MC-*NVT* method with completely random, simultaneous displacements of all atoms and the FA-MC-*NVT* method, where the displacement of each atom is a mixture of a random vector and the force on that atom (FA) with a mixing coefficient chosen such that the efficiency is maximized. The applied temperature versus the MC time for these *NVT* simulations is schematically given in Fig. 1(b).

As can be seen in Fig. 1(c), the behavior of the RA-MC-*NVT* technique and the reference is essentially identical, which suggests that in the present case, it is insignificant if either all or a single atom is randomly displaced. Nevertheless, the straightforward inclusion of nuclear forces in the FA-MC-*NVT* approach leads to an optimization scheme that can easily get trapped in a local minimum and is hence not competitive. On the contrary, in the (m)fHMC-*NVE* method, this is circumvented by the interplay of $dt$ and $C$. On average $dt_{\max} \approx 2$ fs, which is substantially larger than in a conventional MD simulation for carbon and remains approximately constant during the annealing. In this way, the available gradient information is rather well exploited. However, upon rejections, the decrease of $dt$ is counterbalanced by $C$ to conserve the instantaneous total energy and therefore prevents the system from being trapped in a local minimum. In the end, by employing the mfHMC-*NVE* method, the same potential energy as using the RS-MC-*NVT* approach is realized, though with a cooling time that is two orders of magnitude shorter. Comparing the final potential energies with the ground-state energies of diamond ($-7.349$ eV/atom) and graphite ($-7.374$ eV/atom), it is apparent that the eventual structures correspond to amorphous carbon, whose energies are about 0.4 eV/atom above the corresponding ground state.

As already mentioned, the mfHMC-*NVE* method shows the best performance regarding its ability to find low-energy states. On the other side, it is feasible to do much longer simulations (in terms of tee) with the RS-MC-*NVT* method than with the other techniques because the reevaluation of the total energy after the displacement of one single atom is relatively fast for the empirical LCBOPII potential; this is due to the intrinsic local dependencies of the energy contributions in such potentials. Since the curve for RA-MC-*NVT* lies on top of that of the RS-MC-*NVT* technique, the latter is preferred whenever updating the total energy for a single-atom move, which is faster than for an all-atom move.

To illustrate our method, we apply the mfHMC-*NVE* method to minimize Eq. (2) for amorphous carbon at the density functional level of theory (DFT). Therein, $U(\mathbf{R})$ is the total energy from DFT supplemented by the reduced radial distribution function $G(r)$, derived from scattering data, and the optical Tauc gap $\Delta E_{\text{tauc}}$ for amorphous phases.[35,36] Hence, in this case, Eq. (2) takes the form

$$\tilde{U}(\mathbf{R}) = U(\mathbf{R}) + w_G \sum_n \left[G_n(\mathbf{R}) - G_n^{\text{exp}}\right]^2 + w_{\text{gap}}\left[\Delta E_{\text{Tauc}}(\mathbf{R}) - \Delta E_{\text{Tauc}}^{\text{target}}\right]^2, \quad (5)$$

where $G_n(\mathbf{R}) = G(r_n)$ denotes a discretized representation of $G(r)$, which is defined as $G(r) = 4\pi r[c(r) - c_0]$, with $c(r)$ the average (number) density of atoms at a distance $r$ and $c_0$ the overall density. To obtain a smoothened $G(r)$, allowing for the calculation of analytical force contributions that were included in the present simulations, we have computed it for any $r = r_n$ on a grid with a spacing of 0.01 Å between the grid points as

$$G(r) = \frac{1}{r\Delta r}\frac{1}{N}\sum_{i,j}\int_{r-\Delta r/2}^{r+\Delta r/2} P_{ij}(r')dr' - 4\pi r c_0, \quad (6)$$

where $P_{ij}(r)$ is a Gaussian-shaped polynomial of degree 4 within the open interval $(r_{ij} - \Delta r, r_{ij} + \Delta r)$ and $P_{ij}(r) = 0$ otherwise, with $P_{ij}$ and $dP_{ij}/dr$ being continuous at $r = r_{ij} \pm \Delta r$, $\int P_{ij}(r)dr = 1$, and $r_{ij}$ being the interatomic distance between atom $i$ and $j$. The values reported for the experimental gap of amorphous carbon vary between 1.0 and 2.5 eV, possibly depending on the particular sample.[18] Therefore, we have taken an intermediate target value equal to $\Delta E_{\text{tauc}}^{\text{target}} = 1.7$ eV for our simulation. However, in the present study, we have neglected the gradient of the Tauc gap term with respect to $\mathbf{R}$ in the analytic expression of the forces. Nevertheless, using finite

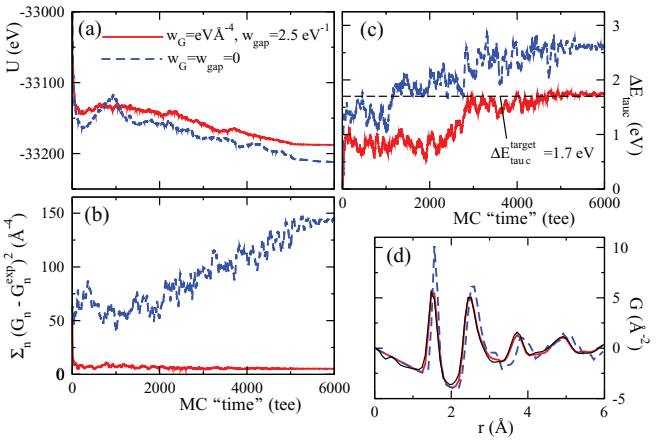


FIG. 2. (Color online) Evolution of the (a) potential energy, (b) sum of the squared residuals of the RDF and (c) Tauc gap as a function of time during the optimization using the mfHMC-*NVE* technique to determine the structure of amorphous carbon. The solid line denotes our simulation method, while the conventional SA approach is depicted by the dashed line. The comparison of the corresponding $G(r)$, as obtained using both techniques, with the experimental one,[34] given by the solid line, is shown in Fig. 2(d). Due to the nearly perfect agreement, the experimental curve is almost completely covered by the results from the present method (red line).

differences, it is straightforward to include them, although at the price that the computation becomes at least a factor of $3N$ times more expensive. Further details on the on-the-fly calculation of the Tauc gap are discussed in the appendix.

Even though the values of the weight factors $w_G$ and $w_{\text{gap}}$ have some importance, their impact is relatively small. In principle, they should be chosen as small as possible and just large enough to get a good agreement with the experimental data. In the present simulation, we have used $w_G = 1$ eV Å$^4$ and $w_{\text{gap}} = 2.5$ eV$^{-1}$. In general, the value $w_G$ should be chosen in such a way that in the beginning of the simulation at high temperature, $w_G \sum_n [G_n(\mathbf{R}) - G_n^{\text{exp}}]^2$ is on the same order of magnitude as the thermal energy $\frac{3}{2} N k_B T$. In contrast, the parameter $w_{\text{gap}}$ can be selected to be considerably smaller than $\frac{3}{2} N k_B T / [\Delta E_{\text{Tauc}}(\mathbf{R}) - \Delta E_{\text{Tauc}}^{\text{target}}]^2$.

We have linked our code to the CP2K suite of programs to compute the necessary total energies and forces.[37] The closed-shell DFT calculations were performed for exactly the same system as before using the Perdew-Burke-Ernzerhof (PBE) exchange-correlation functional[38] and norm-conserving Goedecker-type pseudopotentials.[39] The total-energy schedule applied included an equilibration at $E = -32\,950$ eV for 1000 tee, followed by a cooling from $E = -32\,950$ to $E = -33\,175$ eV during 4000 tee and a final run of length 1000 tee during which $E$ is further lowered to get as close as possible to $\tilde{U}_{f,0}$.

The results of such simulations using our method, with and without the experimental constraints, are presented in Fig. 2 and are compared to a conventional HMC-based SA simulation. The improved overall agreement with the underlying experimental data is apparent, as shown in Figs. 2(c) and 2(d).

We conclude by noting that our method in conjunction with an appropriate minimization procedure has a wide domain of applicability, not confined to amorphous phases. We wish to specifically highlight that the present scheme can be directly applied to any other disordered system, such as liquid water[40] or, including the NMR chemical shift,[41,42] to determine the structure of proteins and nucleic acids. However, the maximum permissible system size is limited by the underlying electronic structure method. Further improvement of the method and the minimizer will be presented elsewhere.

We would like to thank A. Zunger for fruitful discussions, D. Richters for critical reading of the manuscript, as well as the IDEE project of the Carl-Zeiss Foundation and the Graduate School of Excellence MAINZ for financial support.

## APPENDIX: TAUC GAP

The optical Tauc gap $\Delta E_{\text{Tauc}}$ is a convenient definition for the gap of amorphous phases, which circumvents the difficulty that the band structure of disordered systems is not properly defined. It relies on the following relation[36] between the experimental optical gap $\Delta E_{\text{gap}}$ and the optical absorption coefficient $\alpha$ as a function of the photon energy $h\nu$:

$$\alpha(h\nu) h\nu \propto (h\nu - \Delta E_{\text{gap}})^2, \tag{A1}$$

which is applicable to (amorphous) semiconductors within a certain range of photon energies just beyond the gap $\Delta E_{\text{gap}}$. For the on-the-fly calculation of $\Delta E_{\text{Tauc}}$ within each optimization step, we first compute the optical absorption coefficient $\alpha$ from[43]

$$\alpha(h\nu) = \frac{K}{h\nu} \int_{E_F}^{E_F + h\nu} n(E - h\nu) \tilde{n}(E) dE, \tag{A2}$$

where $K$ is a constant, while $n$ and $\tilde{n}$ are the densities of the occupied and unoccupied states, respectively, that are computed from the eigenvalue spectrum of the DFT Hamiltonian after self-consistency has been achieved. Plotting $\sqrt{\alpha(h\nu) h\nu}$ as a function of $h\nu$ within a photon energy range around the gap obeys a linear regime, from which $\Delta E_{\text{Tauc}} = \Delta E_{\text{gap}}$ can be obtained by taking the intersection between the linear fit with the horizontal $\sqrt{\alpha(h\nu) h\nu} = 0$ axis. We note that the value of the constant $K$ is irrelevant for the value of $\Delta E_{\text{Tauc}}$ resulting from this approach. Since the linear behavior only applies to a finite-energy range just beyond the gap, the linear fit has to be restricted to this energy interval. For the automatic computation of $\Delta E_{\text{Tauc}}$, we have selected this interval to be within the interval $[(1 - \Delta) f W_{\text{tot}}, f W_{\text{tot}}]$, where $W_{\text{tot}}$ is the total width of the spectrum.

*kuehne@uni-mainz.de

[1] R. Zallen, *The Physics of Amorphous Solids* (Wiley, New York, 1983).

[2] S. R. Elliott, *Physics of Amorphous Materials* (Longman, Essex, 1990).

[3] W. H. Zachariasen, J. Am. Chem. Soc. **54**, 3841 (1932).

[4]M. Jansen, J. C. Schön, and L. van Wüllen, Angew. Chem. Int. Ed. **45**, 4244 (2006).
[5]J. Maddox, Nature (London) **335**, 6187 (1988).
[6]D. M. Deaven and K. M. Ho, Phys. Rev. Lett. **75**, 288 (1995).
[7]D. J. Wales and H. A. Scheraga, Science **285**, 1368 (1999).
[8]R. Martonak, A. Laio, and M. Parrinello, Phys. Rev. Lett. **90**, 075503 (2003).
[9]S. Goedecker, J. Chem. Phys. **120**, 9911 (2004).
[10]C. W. Glass, A. G. Oganov, and N. Hansen, Comput. Phys. Commun. **175**, 713 (2006).
[11]G. Trimarchi and A. Zunger, Phys. Rev. B **75**, 104113 (2007).
[12]S. C. Woodley and R. Catlow, Nature Mater. **7**, 937 (2008).
[13]C. Wehmeyer, G. F. von Rudorff, S. Wolf, G. Kabbe, D. Schärf, T. D. Kühne, and D. Sebastiani, J. Chem. Phys. **137**, 194110 (2012).
[14]S. Kirkpatrick, C. D. Gelatt, and M. P. Vecchi, Science **220**, 671 (1983).
[15]R. Car and M. Parrinello, Phys. Rev. Lett. **55**, 2471 (1985).
[16]T. D. Kühne, M. Krack, F. R. Mohamed, and M. Parrinello, Phys. Rev. Lett. **98**, 066401 (2007).
[17]J. Sarnthein, A. Pasquarello, and R. Car, Phys. Rev. Lett. **74**, 4682 (1995); Phys. Rev. B **52**, 12690 (1995).
[18]N. A. Marks, D. R. McKenzie, B. A. Pailthorpe, M. Bernasconi, and M. Parrinello, Phys. Rev. Lett. **76**, 768 (1996); Phys. Rev. B **54**, 9703 (1996).
[19]S. Caravati, M. Bernasconi, T. D. Kühne, M. Krack, and M. Parrinello, Appl. Phys. Lett. **91**, 171906 (2007); Phys. Rev. Lett. **102**, 205502 (2009); J. Phys.: Condens. Matter **21**, 255501 (2009); S. Caravati, D. Colleoni, R. Mazzarello, T. D. Kühne, M. Krack, M. Bernasconi, and M. Parrinello, *ibid.* **23**, 265801 (2011); J. H. Los, T. D. Kühne, S. Gabardi, and M. Bernasconi, Phys. Rev. B **87**, 184201 (2013).
[20]M. Farnesi Camellone, T. D. Kühne, and D. Passerone, Phys. Rev. B **80**, 033203 (2009).
[21]R. L. McGreevy and L. Pusztai, Mol. Simul. **1**, 359 (1988).
[22]R. L. McGreevy, J. Phys.: Condens. Matter **13**, R877 (2001).
[23]N. Metropolis, A. W. Rosenbluth, M. N. Rosenbluth, A. H. Teller, and E. Teller, J. Chem. Phys. **21**, 1087 (1953).
[24]S. Kugler, L. Pusztai, L. Rosta, P. Chieux, and R. Bellissent, Phys. Rev. B **48**, 7685 (1993).
[25]G. Opletal, T. Petersen, B. O'Malley, I. Snook, D. G. McCulloch, N. A. Marks, and I. Yarovsky, Mol. Phys. **28**, 927 (2002).
[26]O. Gereben and L. Pusztai, J. Comput. Chem. **33**, 2285 (2012).
[27]A. Franceschetti and A. Zunger, Nature (London) **401**, 60 (1999).
[28]P. N. Keating, Phys. Rev. **149**, 674 (1966).
[29]R. O. Jones and O. Gunnarsson, Rev. Mod. Phys. **61**, 689 (1989).
[30]S. Duane, A. D. Kennedy, B. J. Pendleton, and D. Roweth, Phys. Lett. B **195**, 216 (1987).
[31]J. R. Ray, Phys. Rev. A **44**, 4061 (1991).
[32]J. H. Los, L. M. Ghiringhelli, E. J. Meijer, and A. Fasolino, Phys. Rev. B **72**, 214102 (2005).
[33]L. M. Ghiringhelli, J. H. Los, A. Fasolino, and E. J. Meijer, Phys. Rev. B **72**, 214103 (2005).
[34]K. W. R. Gilkes, P. H. Gaskell, and J. Robertson, Phys. Rev. B **51**, 12303 (1995).
[35]K. A. F. Röhrig and T. D. Kühne, Phys. Rev. E **87**, 045301 (2013).
[36]J. Tauc, A. Menth, and D. L. Wood, Phys. Rev. Lett. **25**, 749 (1970).
[37]J. VandeVondele, M. Krack, F. Mohamed, M. Parrinello, T. Chassaing, and J. Hutter, Comput. Phys. Commun. **167**, 103 (2005).
[38]J. P. Perdew, K. Burke, and M. Ernzerhof, Phys. Rev. Lett. **77**, 3865 (1996).
[39]S. Goedecker, M. Teter, and J. Hutter, Phys. Rev. B **54**, 1703 (1996).
[40]T. D. Kühne, M. Krack, and M. Parrinello, J. Chem. Theory Comput. **5**, 235 (2009); T. D. Kühne, T. A. Pascal, E. Kaxiras, and Y. Jung, J. Phys. Chem. Lett. **2**, 105 (2011); T. A. Pascal, D. Schärf, Y. Jung, and T. D. Kühne, J. Chem. Phys. **137**, 244507 (2012); T. D. Kühne and R. Z. Khaliullin, Nature Commun. **4**, 1450 (2013).
[41]F. Mauri, B. G. Pfrommer, and S. G. Louie, Phys. Rev. Lett. **77**, 5300 (1996); **79**, 2340 (1997).
[42]D. Sebastiani and M. Parrinello, J. Phys. Chem. A **105**, 1951 (2001); Phys. Chem. Chem. Phys. **3**, 675 (2002).
[43]R. Bouzerar, C. Amory, A. Zeinert, M. Benlahsen, B. Racine, O. Durand-Drouhin, and M. Clin, J. Non-Cryst. Solids **281**, 171 (2001).